Supporting Information. Doak, D.F., E. Waddle, R.E. Langendorf, A.M. Louthan, N.I. Chardon, R.R. Dibner, D.A. Keinath, E. Lombardi, C. Steenbock, R.K. Shriver, C. Linares, M.B. Garcia, W.C. Funk, S.W. Fitzpatrick, W.F. Morris, and M.L. Peterson. 2021. A critical comparison of integral projection and matrix projection models for demographic analysis. Ecological Monographs.

Table S1. Modeling details for each of the five species.

Species	State variable	survival	mean growth	growth variance	probability of reproduction	propagules, fruits or other units of reproduction produced	Other vital rates used in models:
		Size-dependent vital rates directly fit to data in different ways in our simulations:					
Polygonum viviparum	Sqrt(leaf area)	X	X	X	X	X	bulblings/bulbil*, size distibution of bulblings
Paramuricea clavata	Height	X	X	X			gonads produced per colony size, oocytes/gonad, survival of oocyte to be seen as **recruit**, size distribution of recruits, survival of first year recruits
Vulpicida pinastri	Sqrt(thallus area)	X	X	X			recruits produced per thallus size*, size distribution of recruits
Borderea chouardii	Leaf length	X	X	X	X	X	seeds/fruit, seeds surviving dormant*, seedlings/seed*, size distribution of seedlings

Poecilia reticulata	Wet mass	X	X	X	X	X	Size distribution of offspring

* in all cases, recruits produced per propagule or per parent include survival to be seen in one year after reproduction.

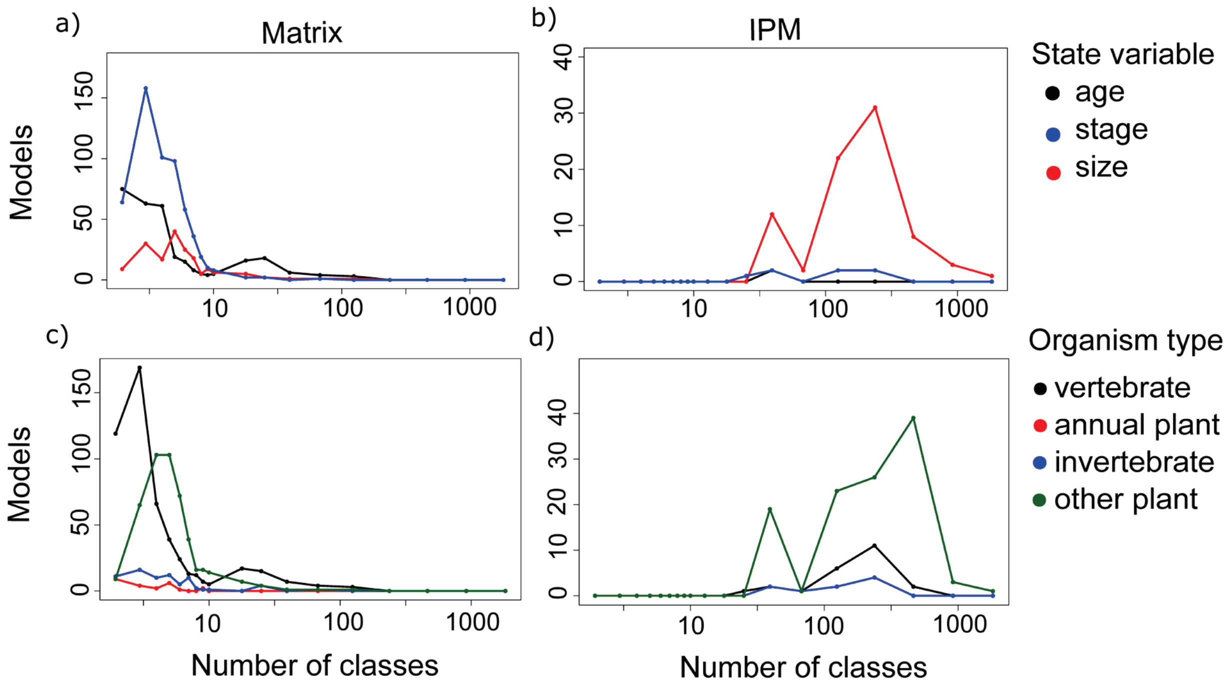

Figure S1. Distribution of class numbers for matrix models (A,C) and IPMs (B,D) with different state variables and for different organisms. Note that models with multiple state variables (e.g., age and size) are not shown here. The data shown are histograms values connected by lines.

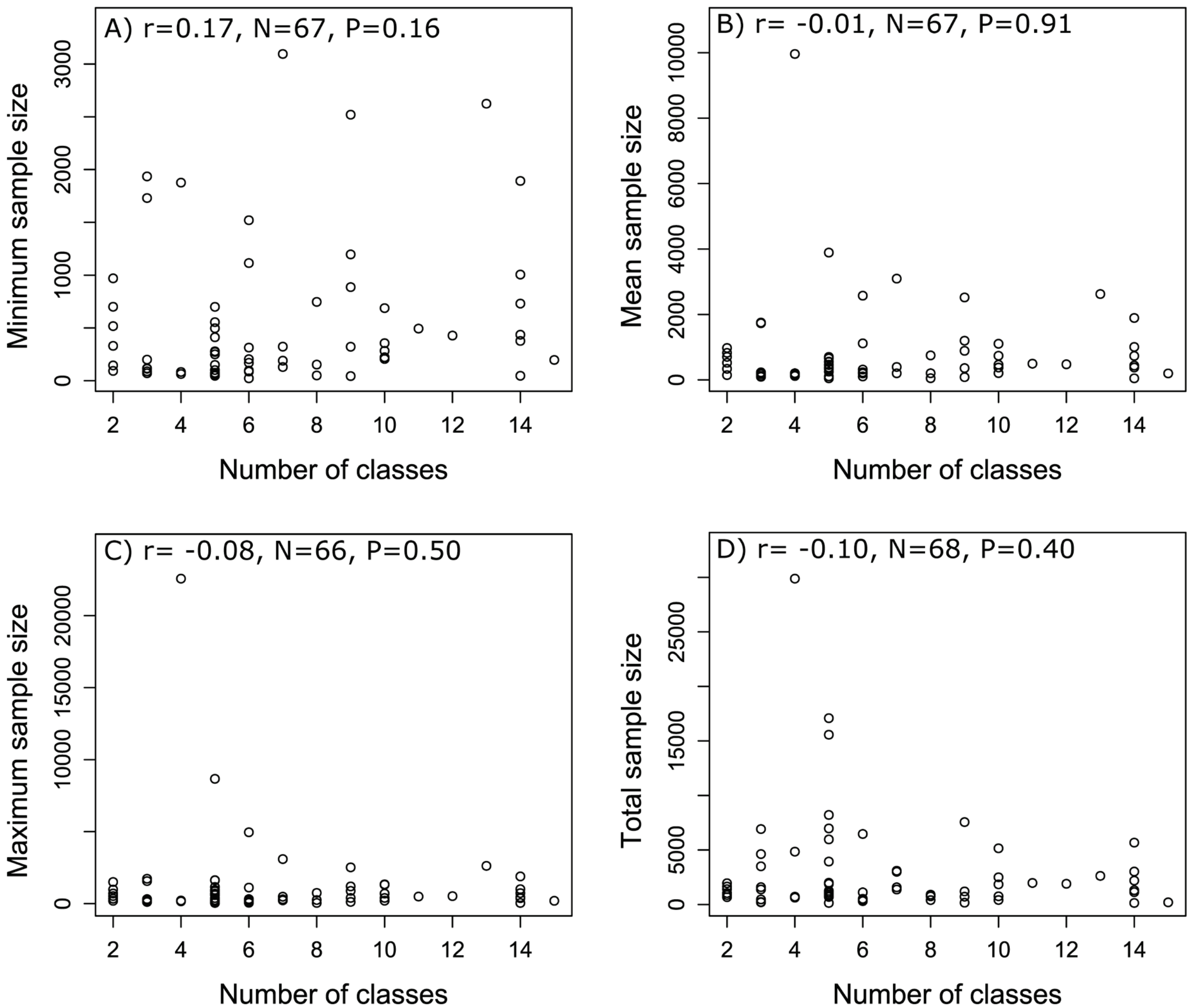

Figure S2: Relationship between sample size and number of classes for size-based matrix models with discrete vital rate estimation found in literature survey. We find no evidence that matrix model dimension is strongly shaped by sample size, as might be expected. We do not include stochastic matrix models, due to the difficulty in characterizing appropriate sample sizes per year or environment, or models with stage or age-based classes since these may be largely determined by species' biology. Sample sizes for a study were most often reported as 1) a range of values for different sites, years, or treatments that were used to construct separate matrices, or 2) a total sample size for the study as a whole. When sample sizes for each matrix were available, we recorded the A) minimum, B) mean, and C) maximum values (note that these are the same when a study includes a single matrix), as well as D) their sum or reported total sample size. Many studies used a different, more limited data set to infer fecundity (and often for only a subset of classes), so we focused on sample sizes used to estimate survival and growth rates across all classes. See Fig. S26 for histograms of these sample sizes.

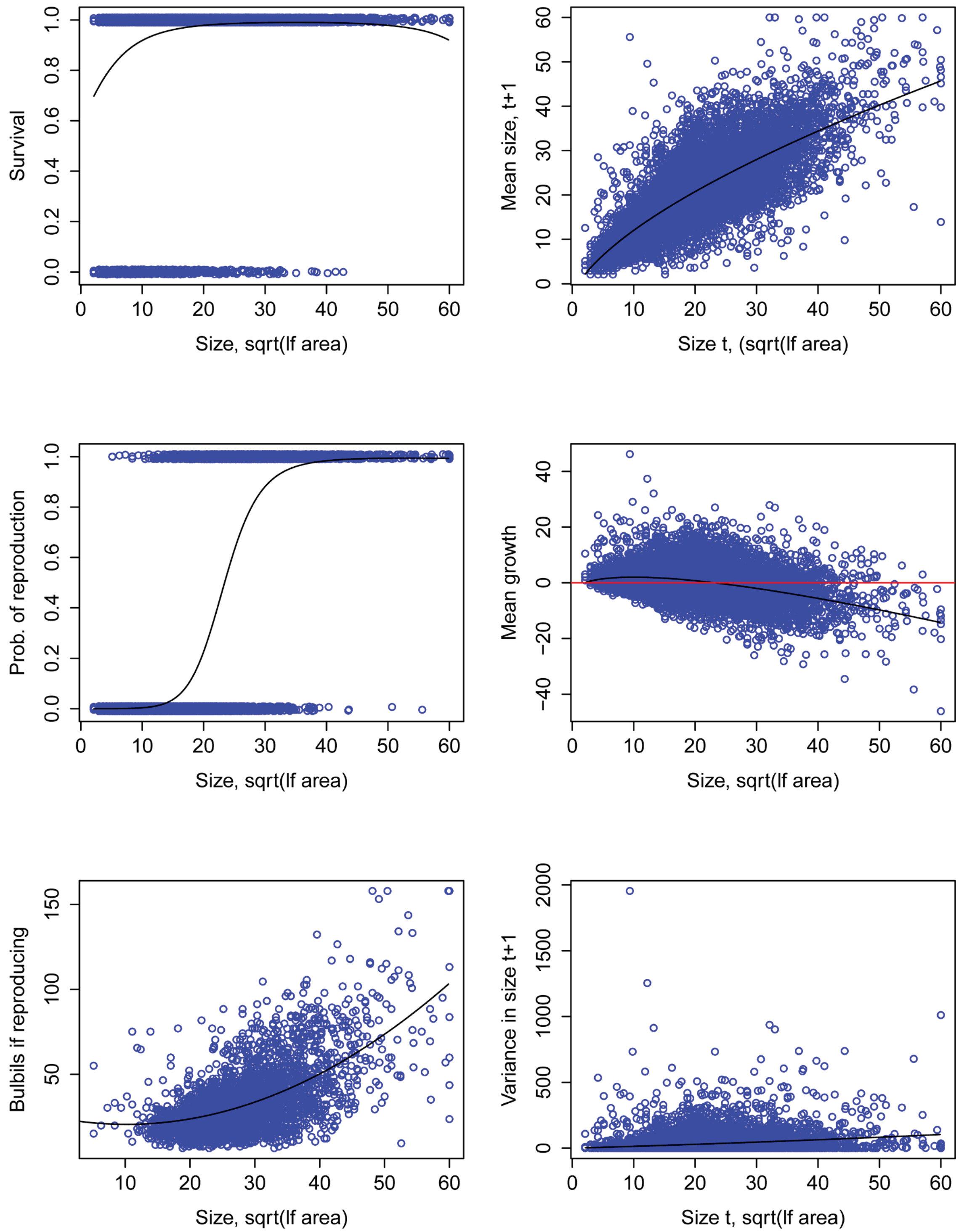

Figure S3. Data and best supported vital rate functions for bistorts. Mean growth is the difference between size t+1 and size t, with the red line indicating no change in size.

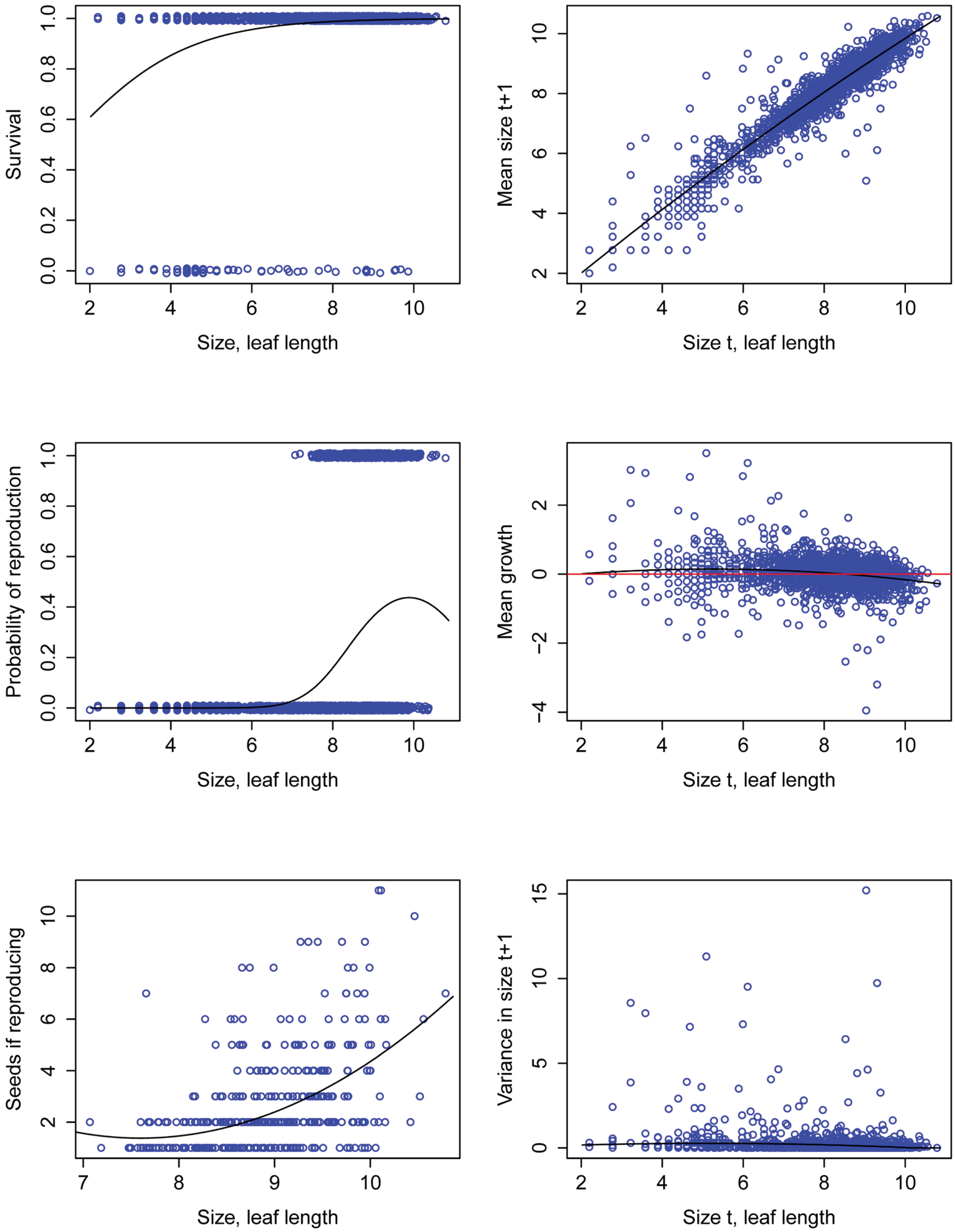

Figure S4. Data and best supported vital rate functions for *Borderea*. Mean growth is the difference between size t+1 and size t, with the red line indicating no change in size.

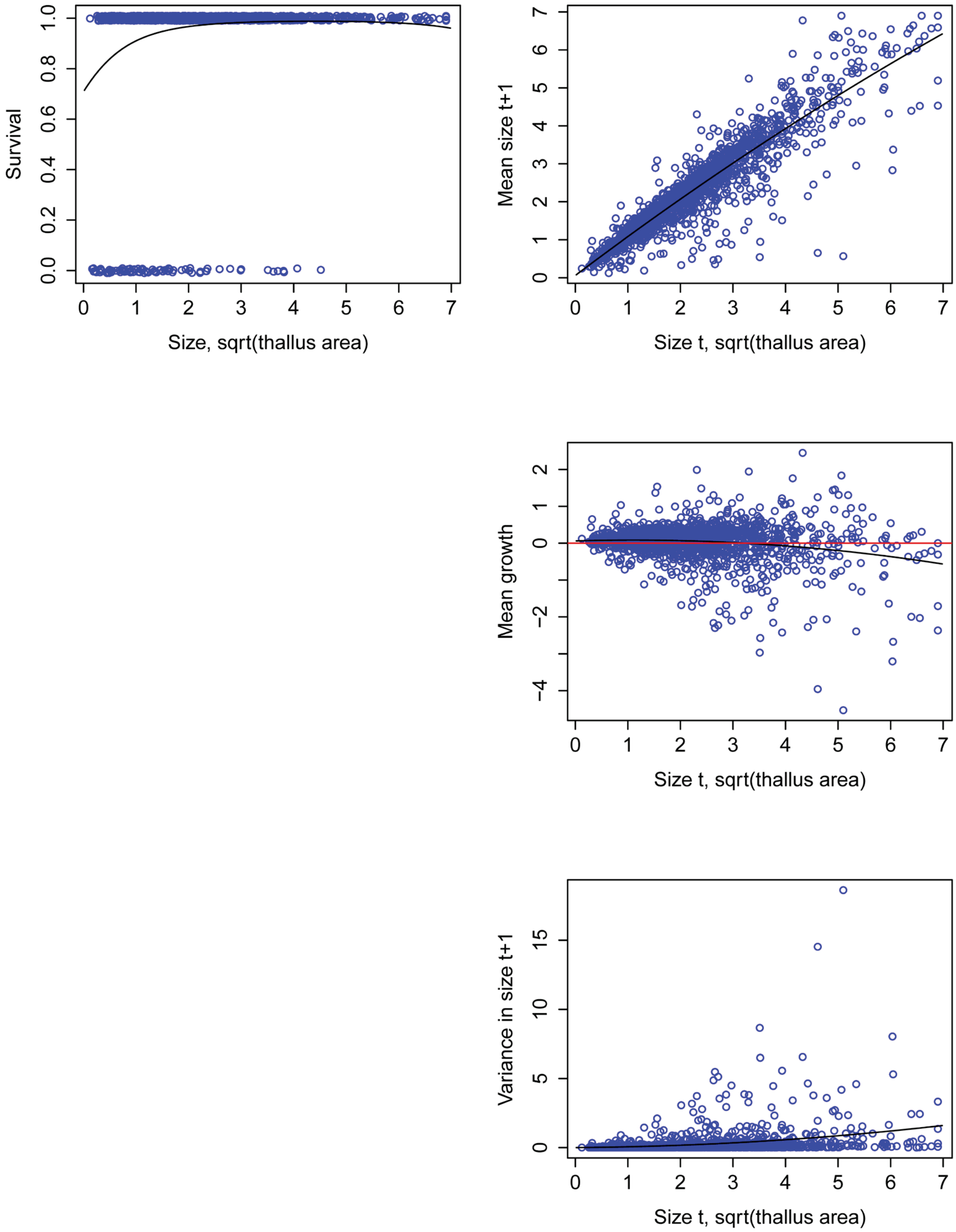

Figure S5. Data and best supported vital rate functions for *Vulpicida*. Mean growth is the difference between size t+1 and size t, with the red line indicating no change in size.

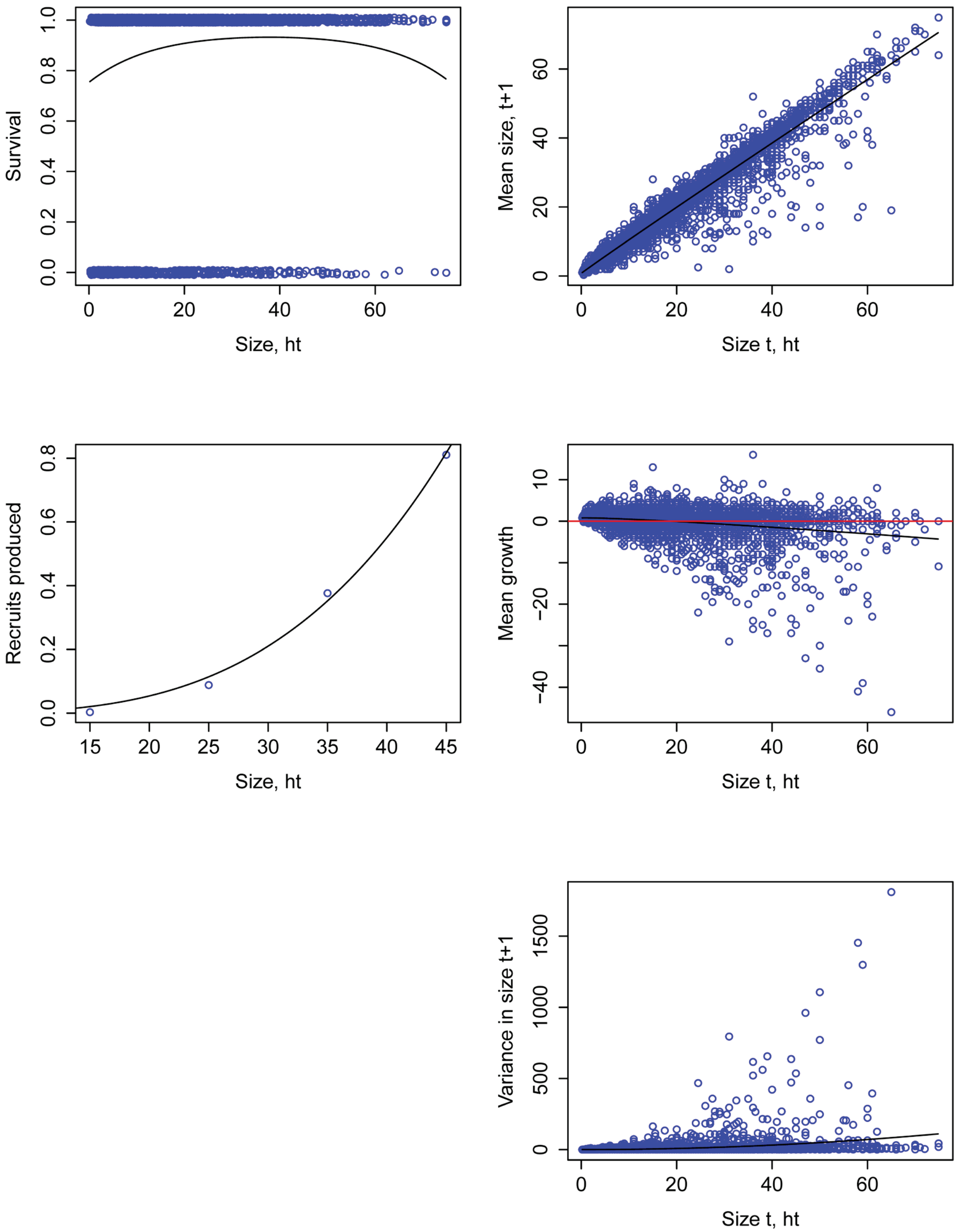

Figure S6. Data and best supported vital rate functions for gorgonians. Mean growth is the difference between size t+1 and size t, with the red line indicating no change in size.

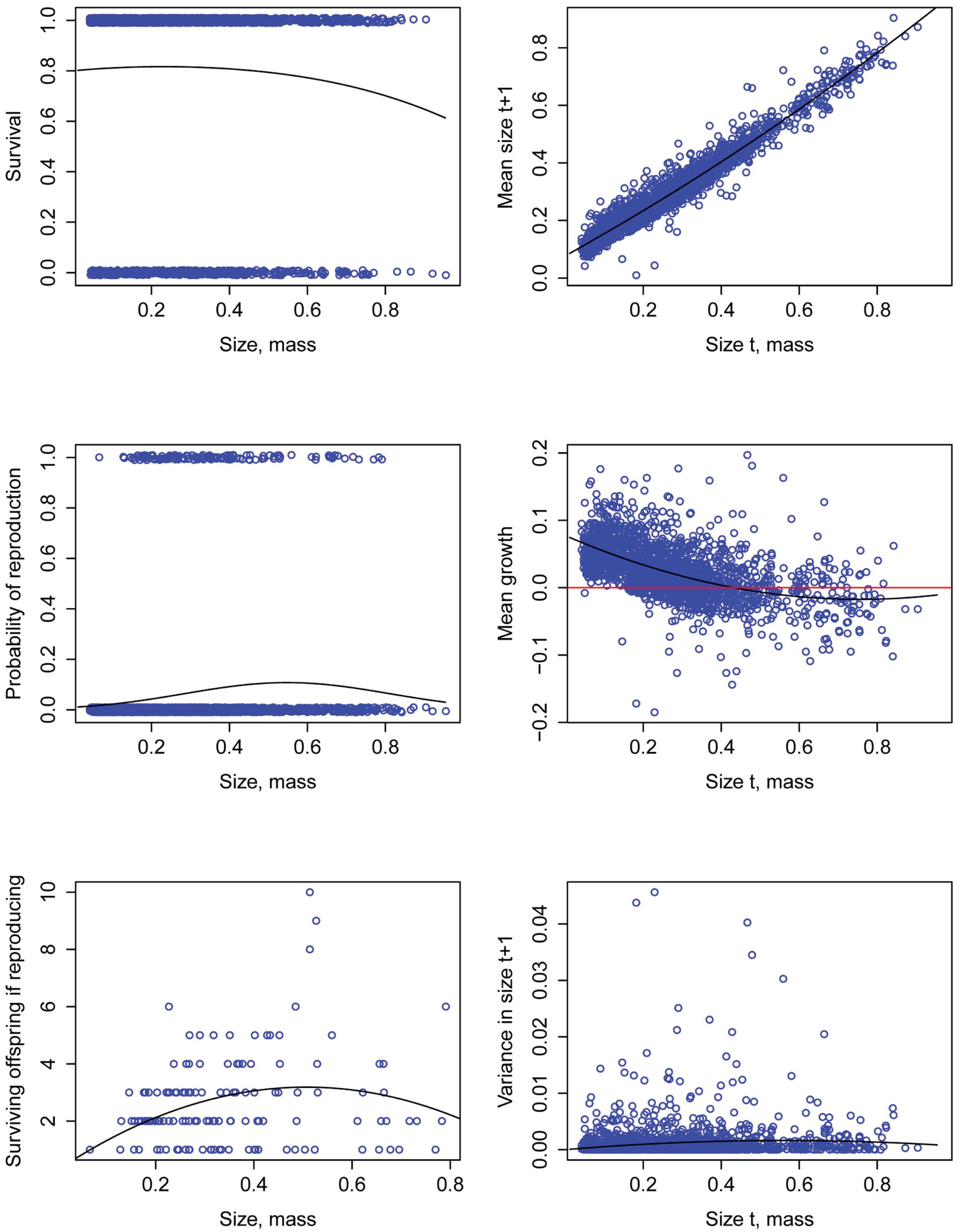

Figure S7. Data and best supported vital rate functions for guppies. Mean growth is the difference between size t+1 and size t, with the red line indicating no change in size.

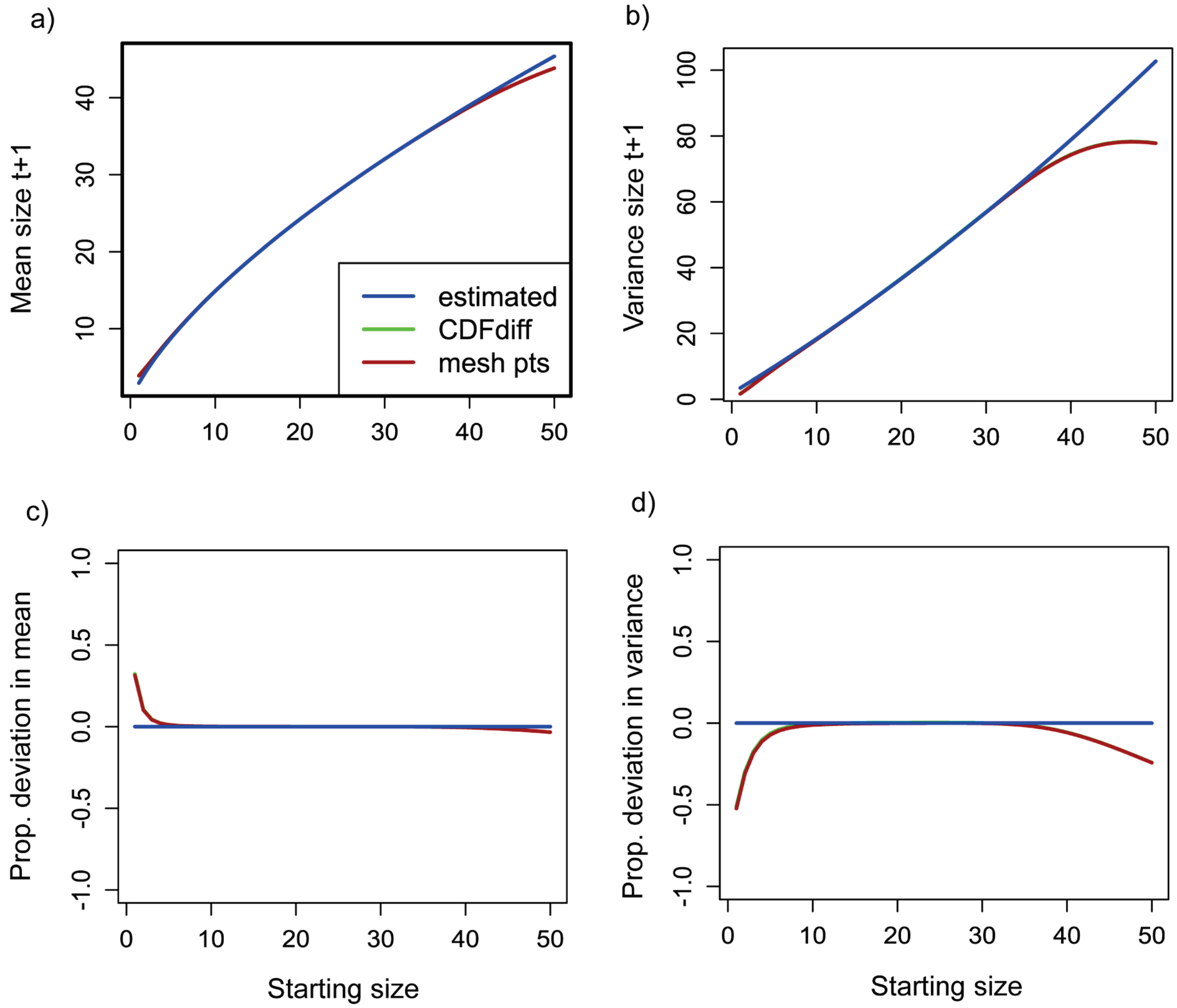

Figure S8. Effects of eviction correction on the mean and variance of size-dependent growth for bistorts. Blue line shows the best estimated relationship between size and the mean (a) or variance (b) of growth. Red and green lines show the relationships following correction for eviction for mesh point and CDF difference estimates of growth, respectively. Note that for bistorts, there is no perceivable difference in the corrected relationships, so the CDF difference and mesh point lines entirely overlap. (c) and (d) show the proportional deviation of mean and variance estimates post correction from the originally estimated relationships.

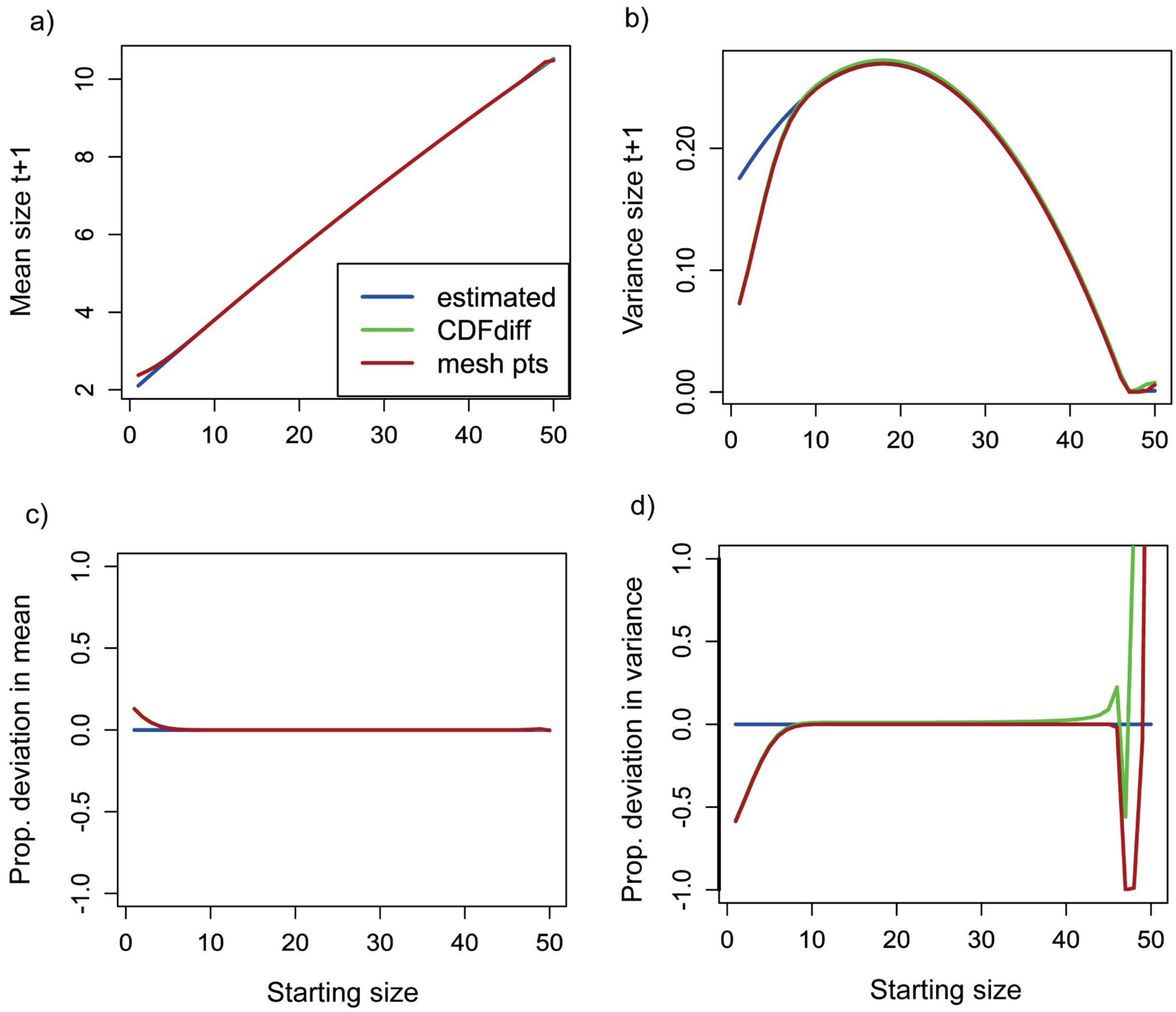

Figure S9. Effects of eviction correction on the mean and variance of size-dependent growth for *Borderea*. Blue line shows the best estimated relationship between size and the mean (a) or variance (b) of growth. Red and green lines show the relationships following correction for eviction for mesh point and CDF difference estimates of growth, respectively. (c) and (d) show the proportional deviation of mean and variance estimates post correction from the originally estimated relationships.

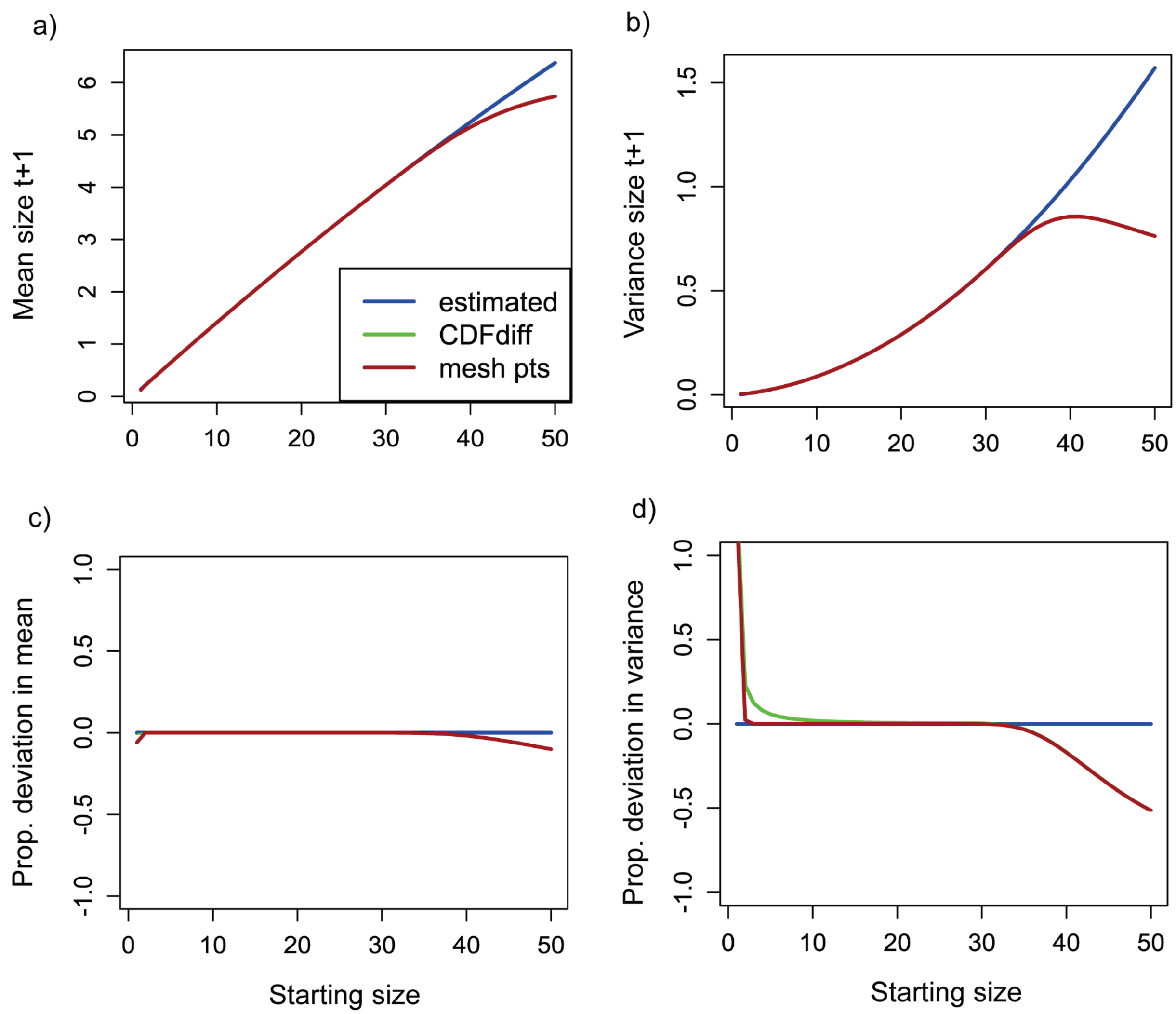

Figure S10. Effects of eviction correction on the mean and variance of size-dependent growth for *Vulpicida*. Blue line shows the best estimated relationship between size and the mean (a) or variance (b) of growth. Red and green lines show the relationships following correction for eviction for mesh point and CDF difference estimates of growth, respectively. Note that there is no perceivable difference in the corrected relationships over much of the range of sizes. (c) and (d) show the proportional deviation of mean and variance estimates post correction from the originally estimated relationships.

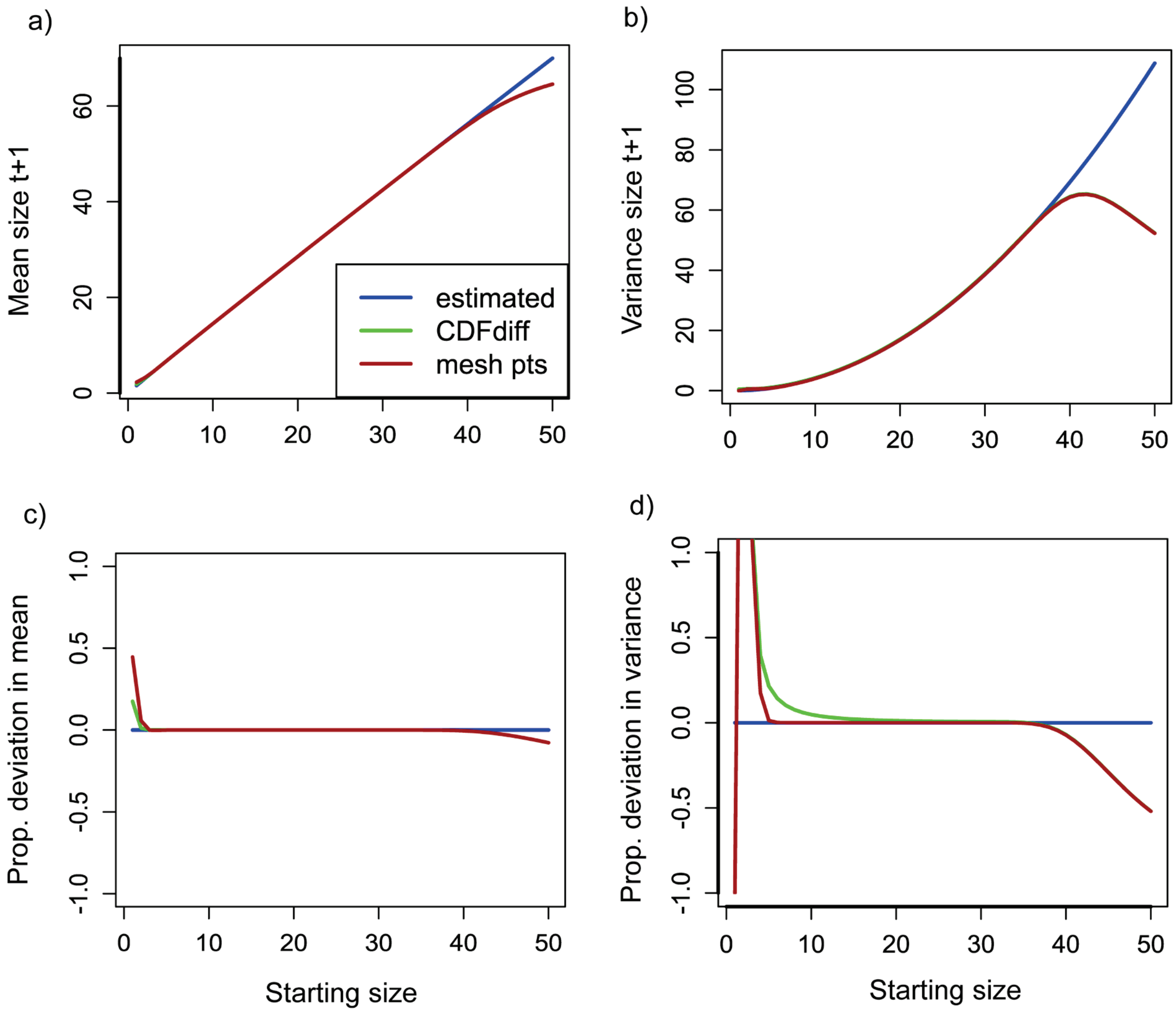

Figure S11. Effects of eviction correction on the mean and variance of size-dependent growth for gorgonians. Blue line shows the best estimated relationship between size and the mean (a) or variance (b) of growth. Red and green lines show the relationships following correction for eviction for mesh point and CDF difference estimates of growth, respectively. Note that there is no perceivable difference in the corrected relationships over much of the range of sizes. (c) and (d) show the proportional deviation of mean and variance estimates post correction from the originally estimated relationships.

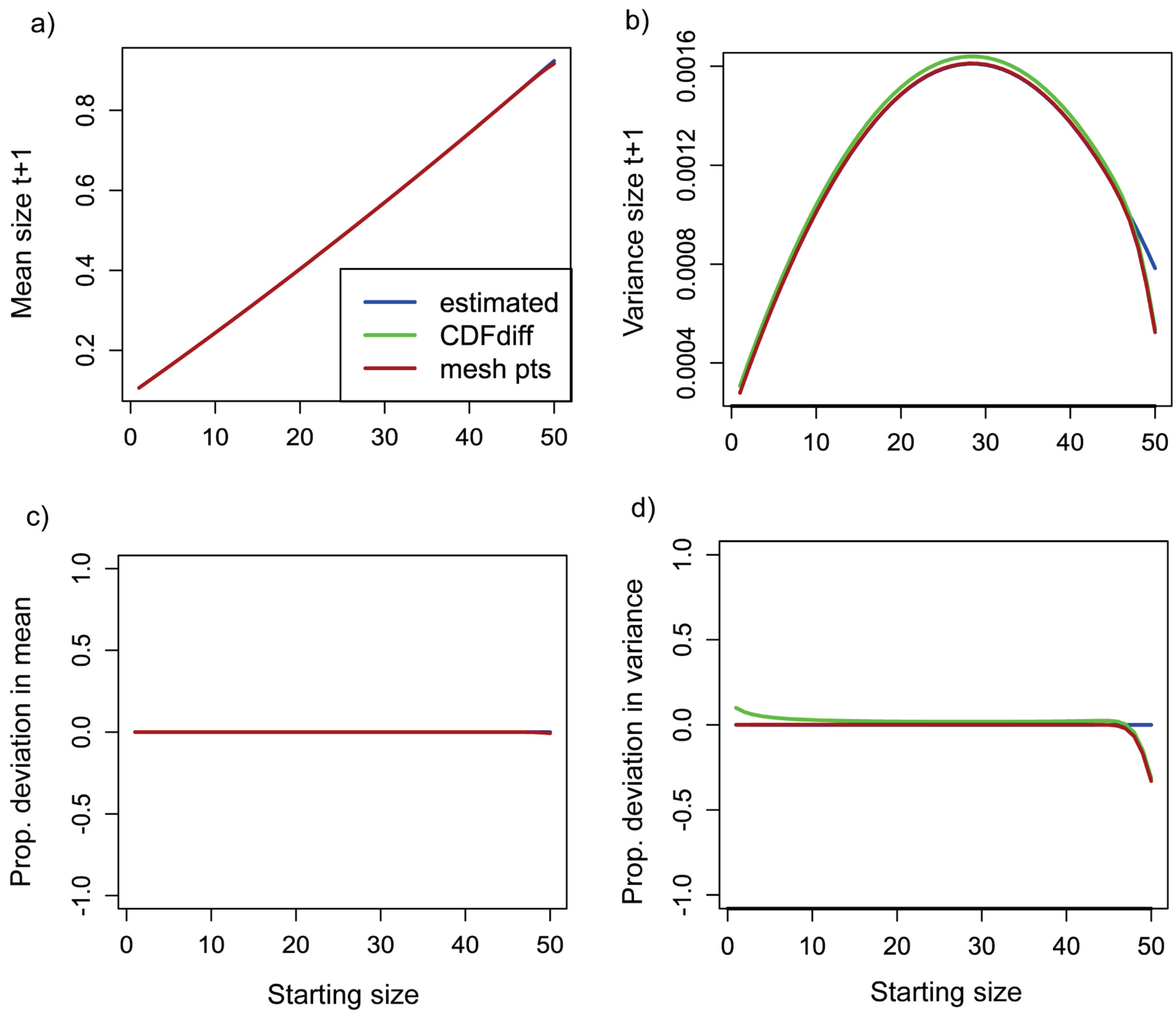

Figure S12. Effects of eviction correction on the mean and variance of size-dependent growth for guppies. Blue line shows the best estimated relationship between size and the mean (a) or variance (b) of growth. Red and green lines show the relationships following correction for eviction for mesh point and CDF difference estimates of growth, respectively. Note that there is no perceivable difference in the corrected relationships over much of the range of sizes. (c) and (d) show the proportional deviation of mean and variance estimates post correction from the originally estimated relationships.

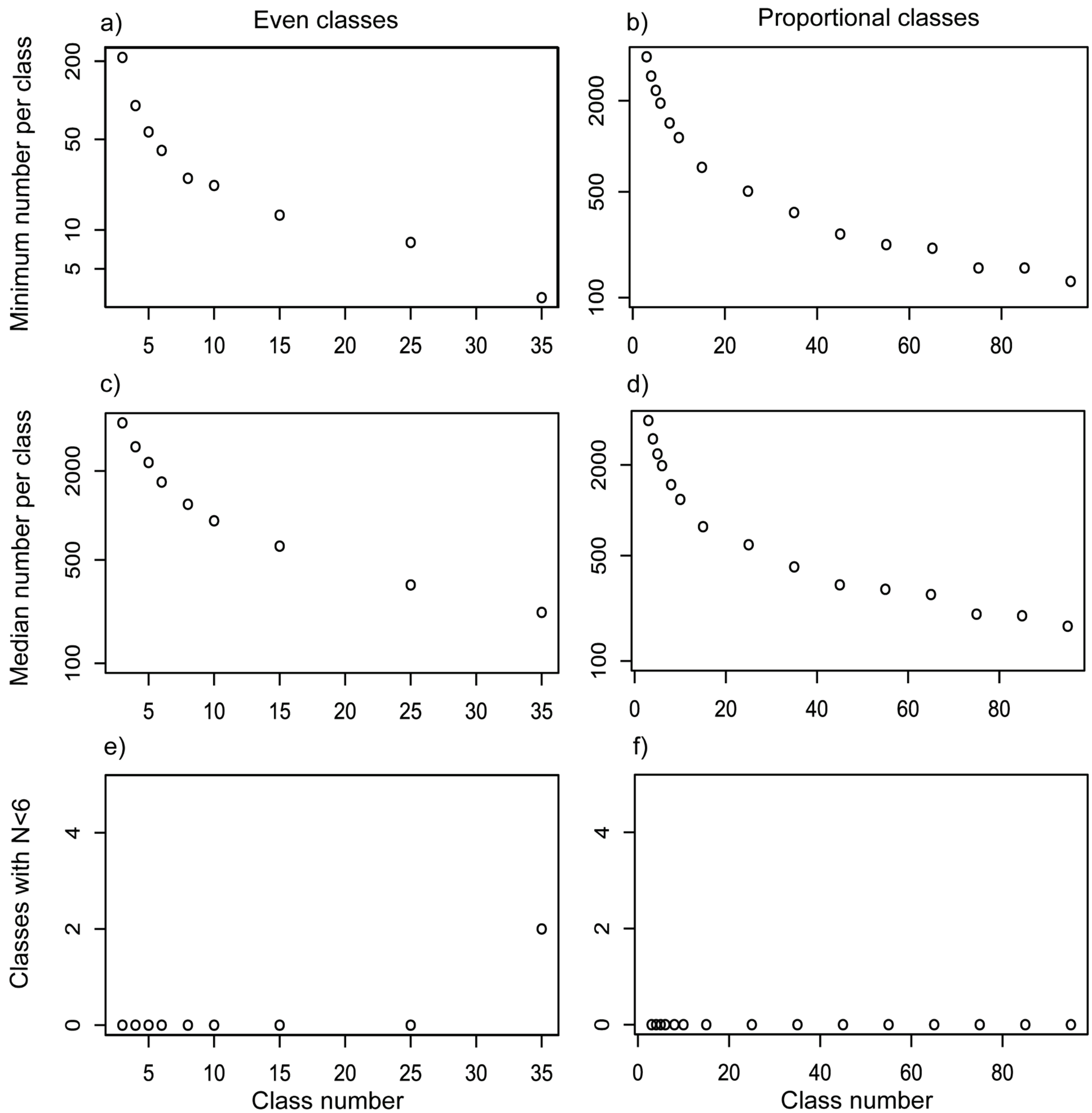

Figure S13. Class-specific sample size summaries for main bistort simulation results (presented in Figures 10-12 in main text).

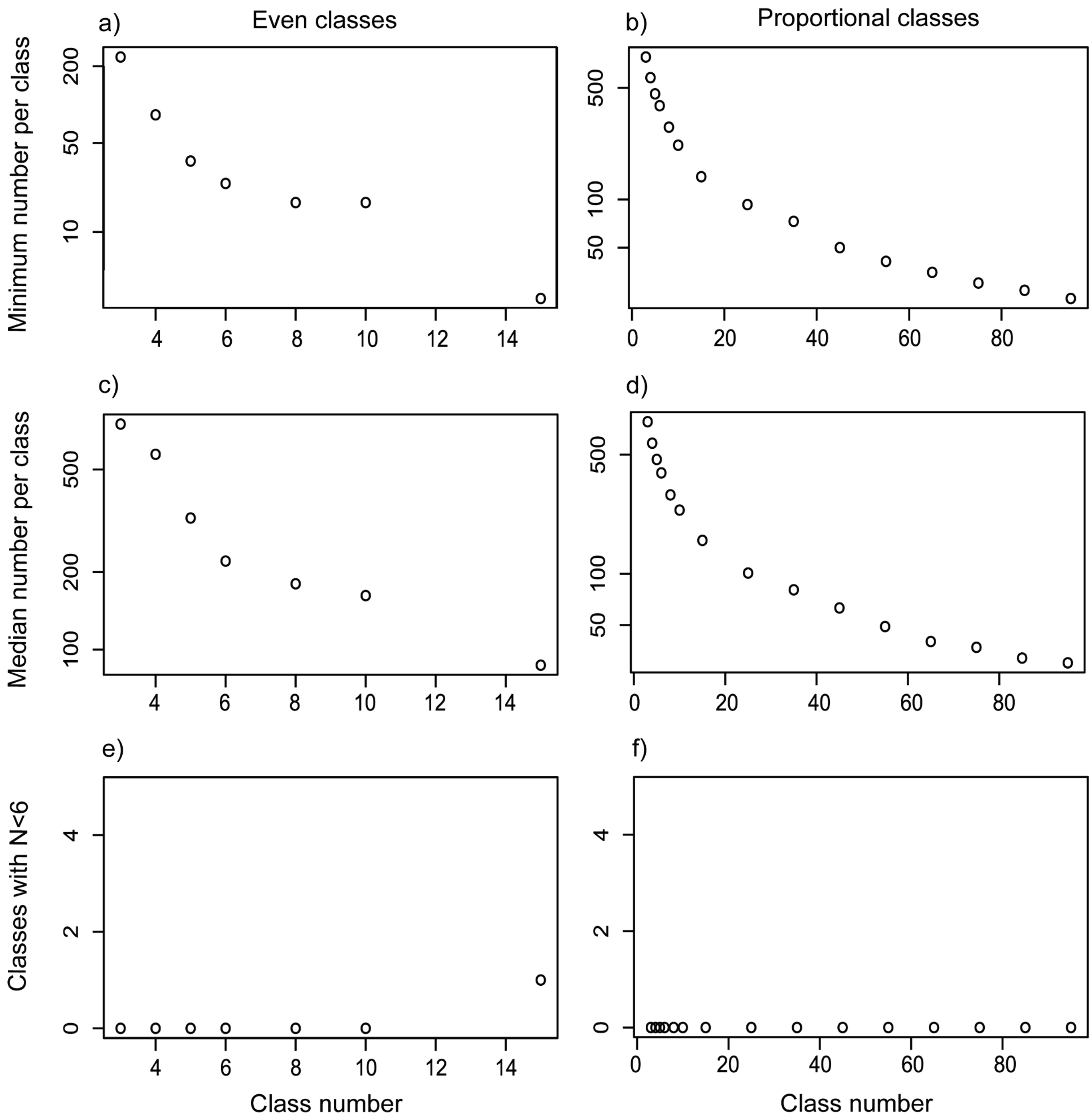

Figure S14. Class-specific sample size summaries for main *Borderea* simulation results (presented in Figures 10-12 in main text).

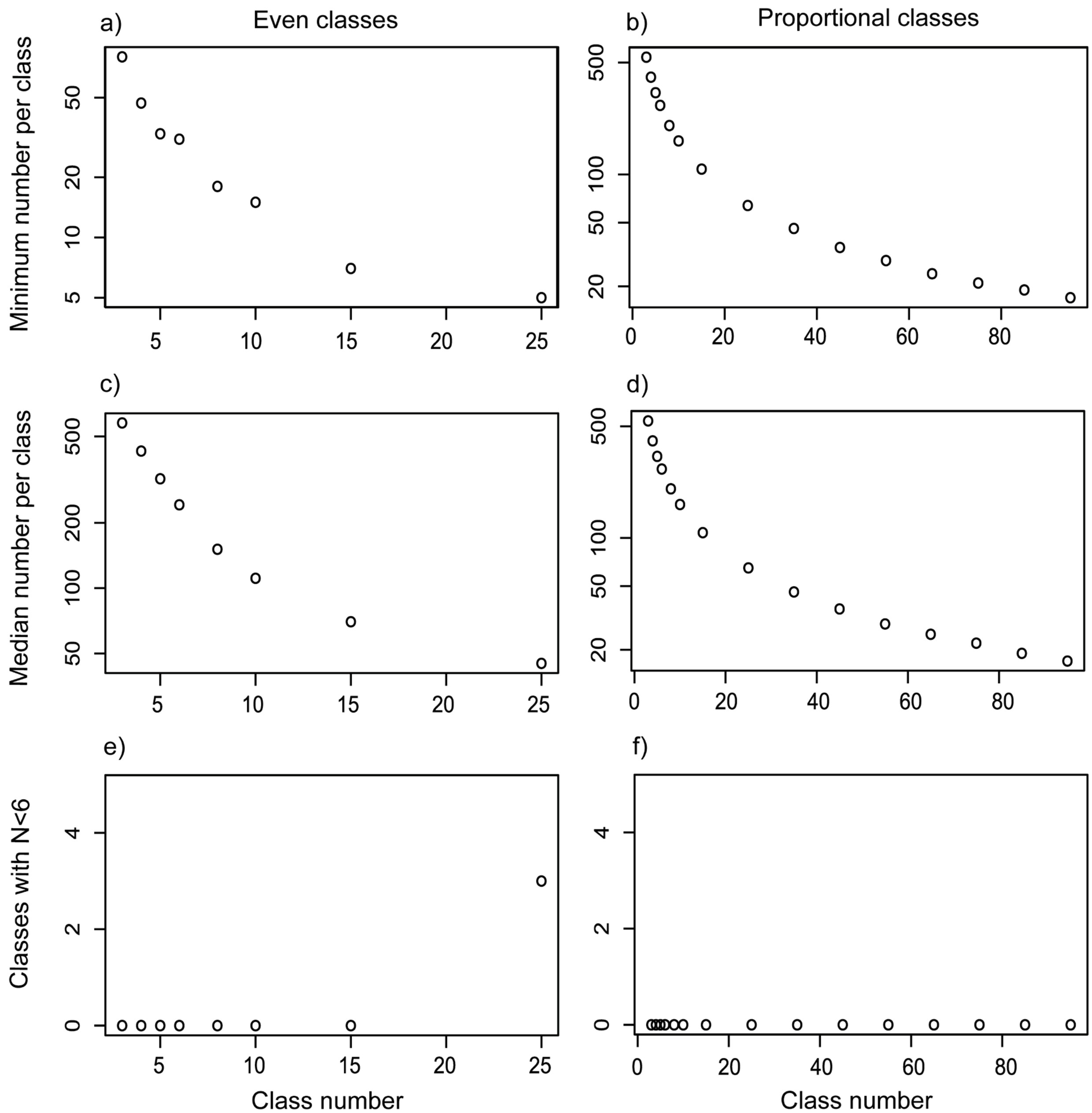

Figure S15. Class-specific sample size summaries for main *Vulpicida* simulation results (presented in Figures 10-12 in main text).

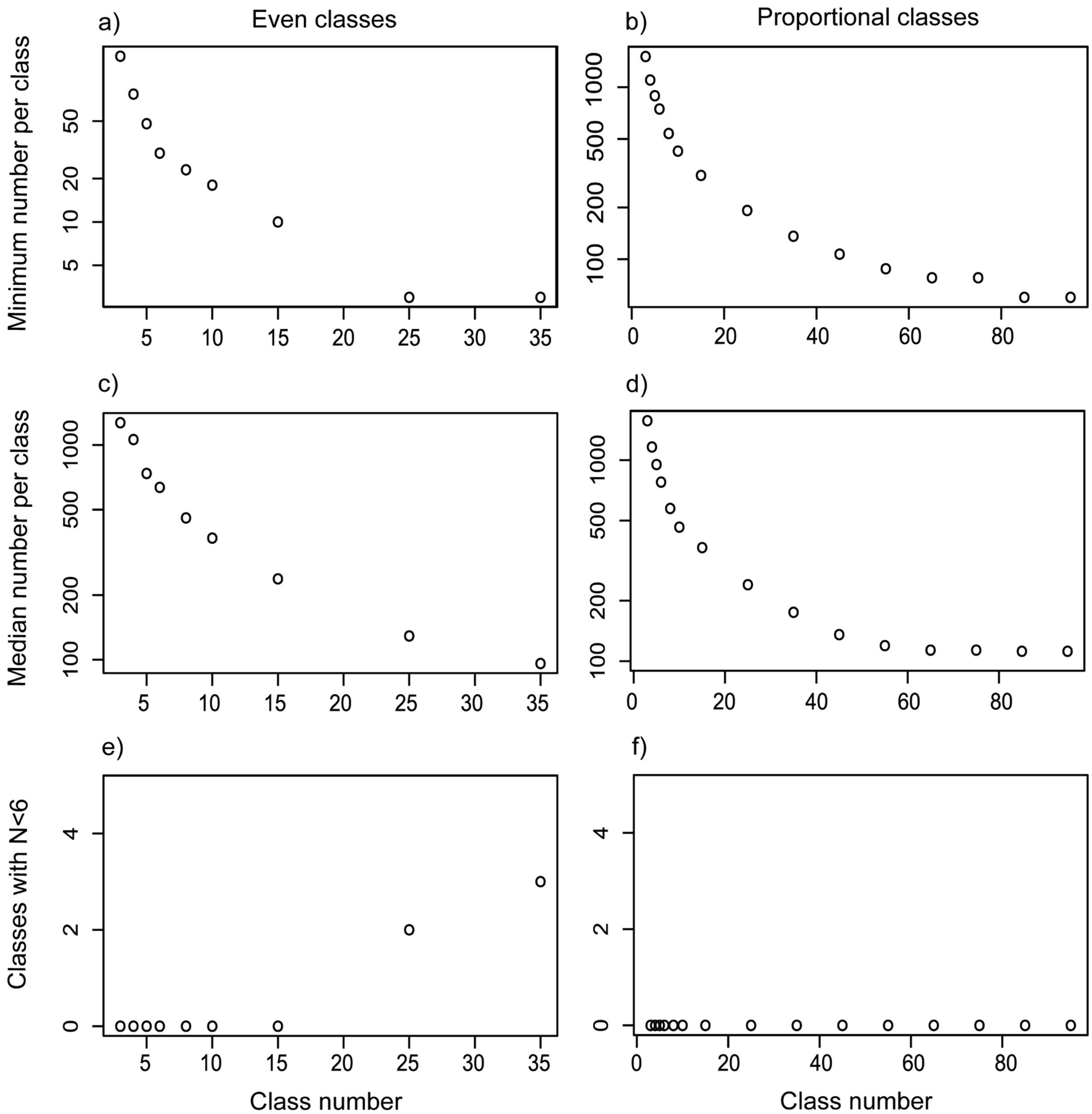

Figure S16. Class-specific sample size summaries for main gorgonian simulation results (presented in Figures 10-12 in main text).

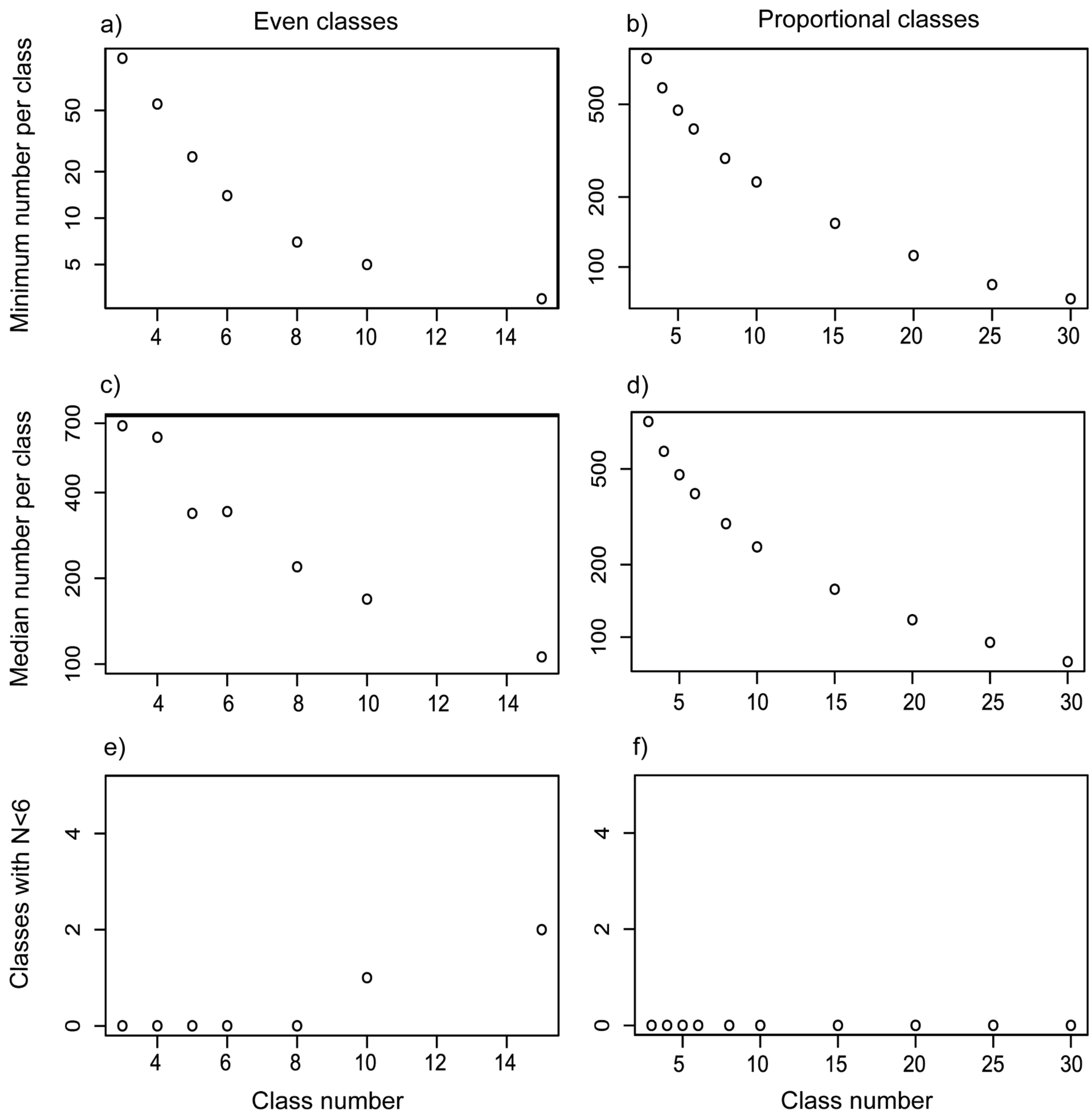

Figure S17. Class-specific sample size summaries for main guppy simulation results (presented in Figures 10-12 in main text).

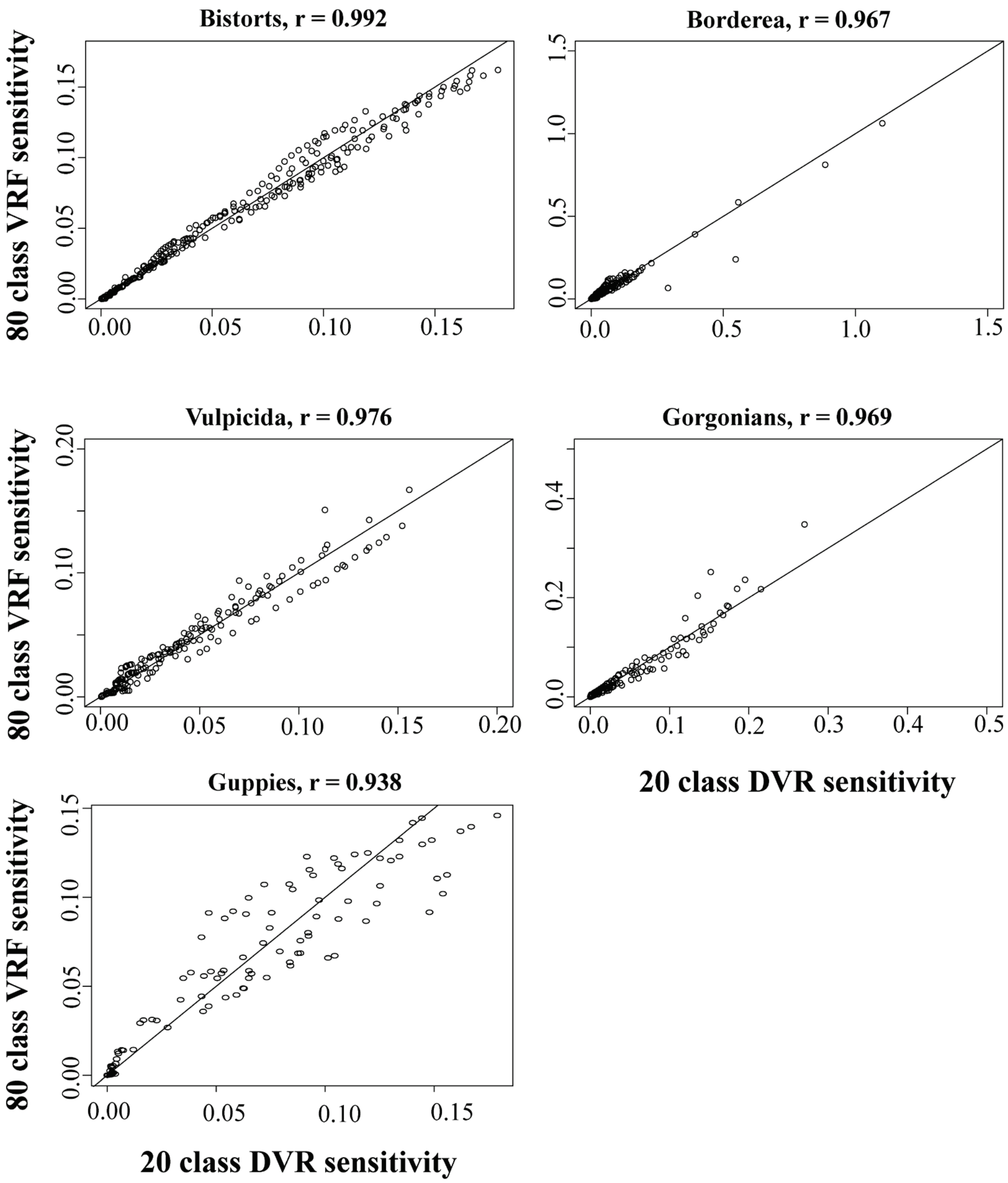

Figure S18. Comparison of sensitivity values for elements in a 20 class DVR model and those from an 80 class CVR model. To condense values from the larger model, we summed sets of sensitivities in each column of the matrix that corresponded to a single, broader category in the smaller model, and then took the average of these values across columns corresponding to the categories in the smaller model. We only compare sensitivities for non-zero matrix elements. Pearson correlation coefficients are shown for each relationship, and lines give the 1:1 slope.

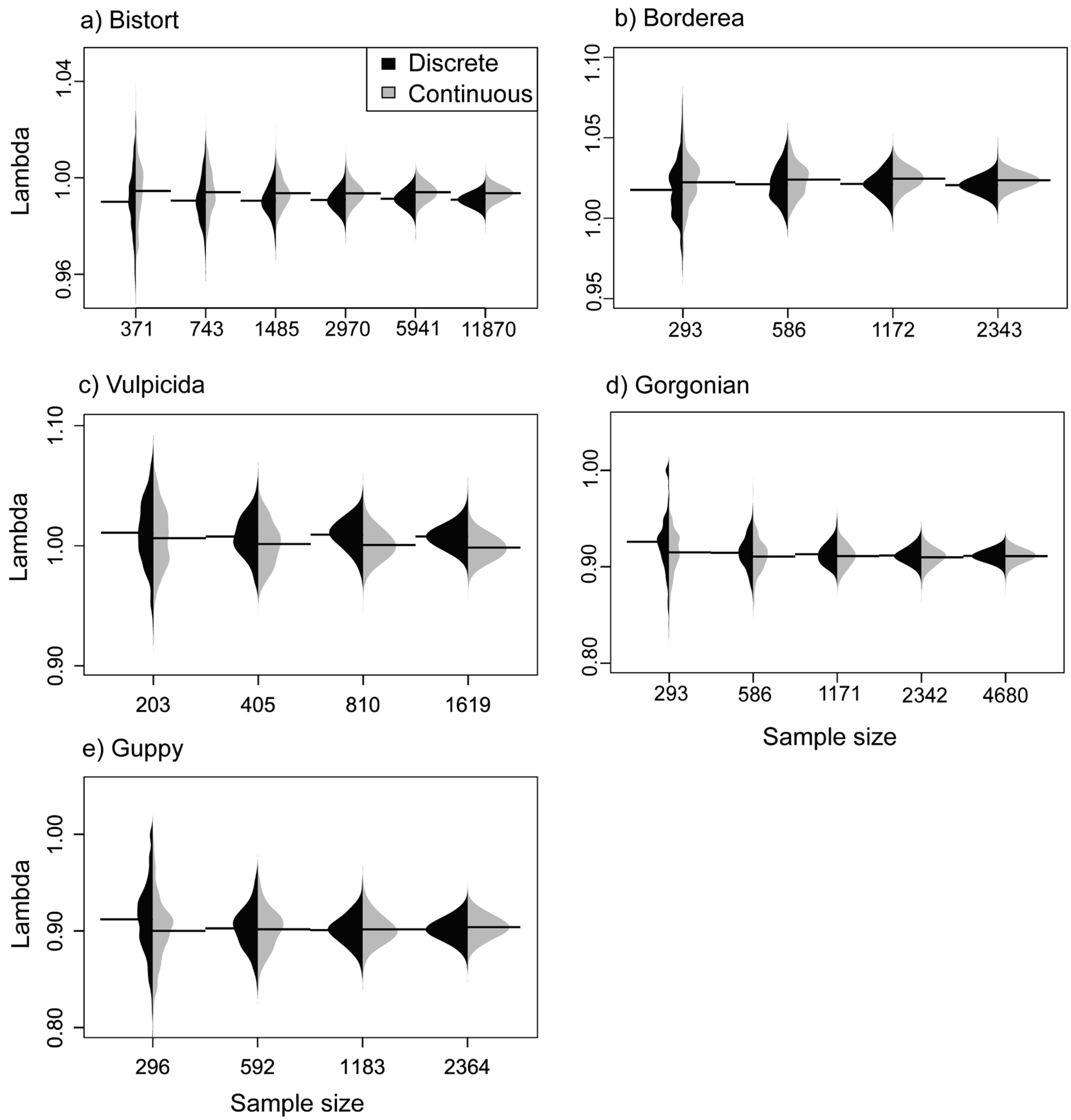

Figure S19. Contrasting distributions of lambda estimates based on bootstrapped, rarified data sets. Discrete models are build using 20 even size classes, while results shown here for continuous models use 80 even classes. Results are nearly identical to those shown in Figure 14 for 20 class continuous models. The horizontal line running through each distribution shows the mean.

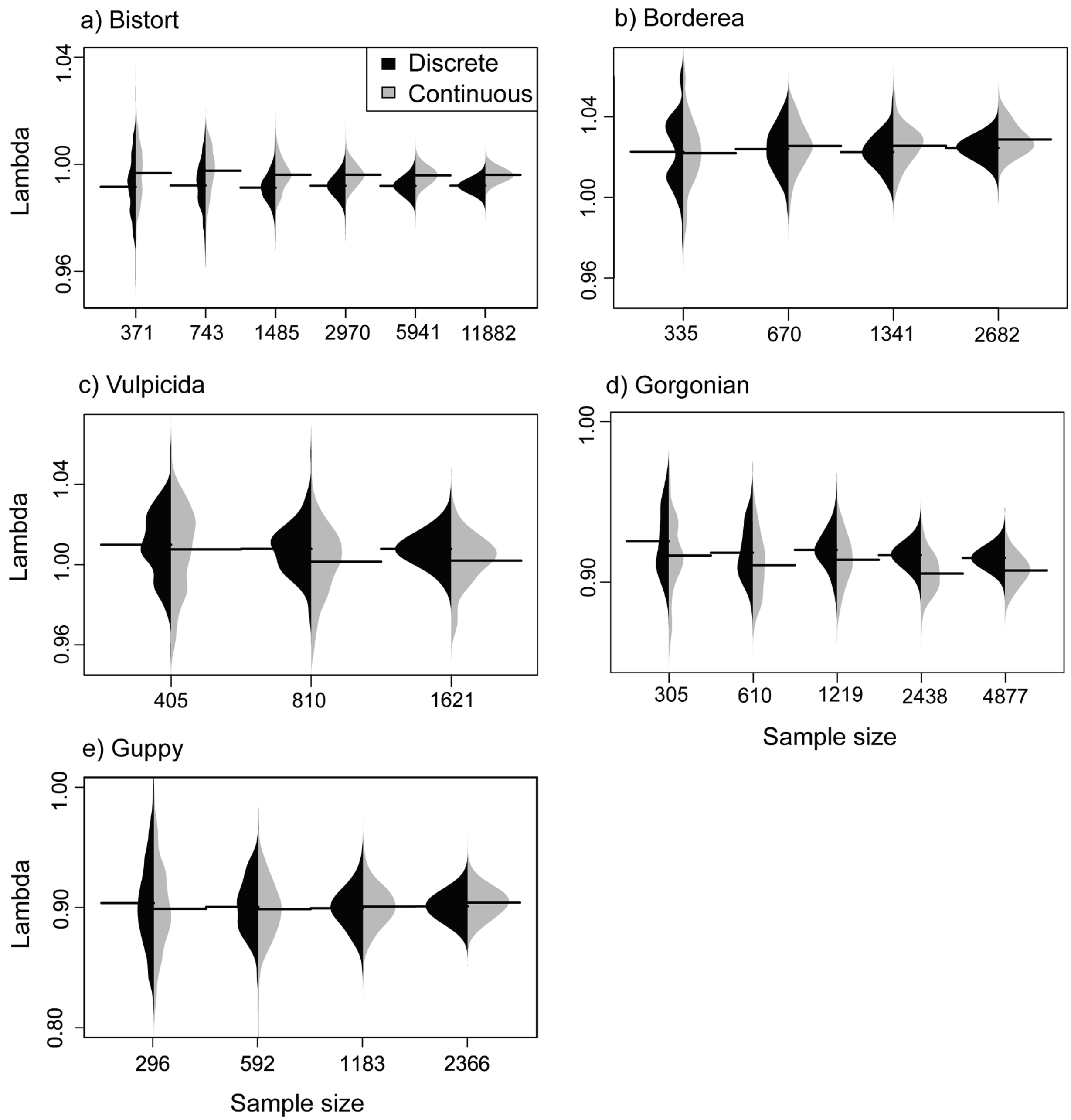

Figure S20. Contrasting distributions of lambda estimates based on simple bootstrapped, rarified data sets and using proportional size classes. Discrete models are build using 20 even size classes, while continuous models use 80 even classes. The horizontal line running through each distribution shows the mean.

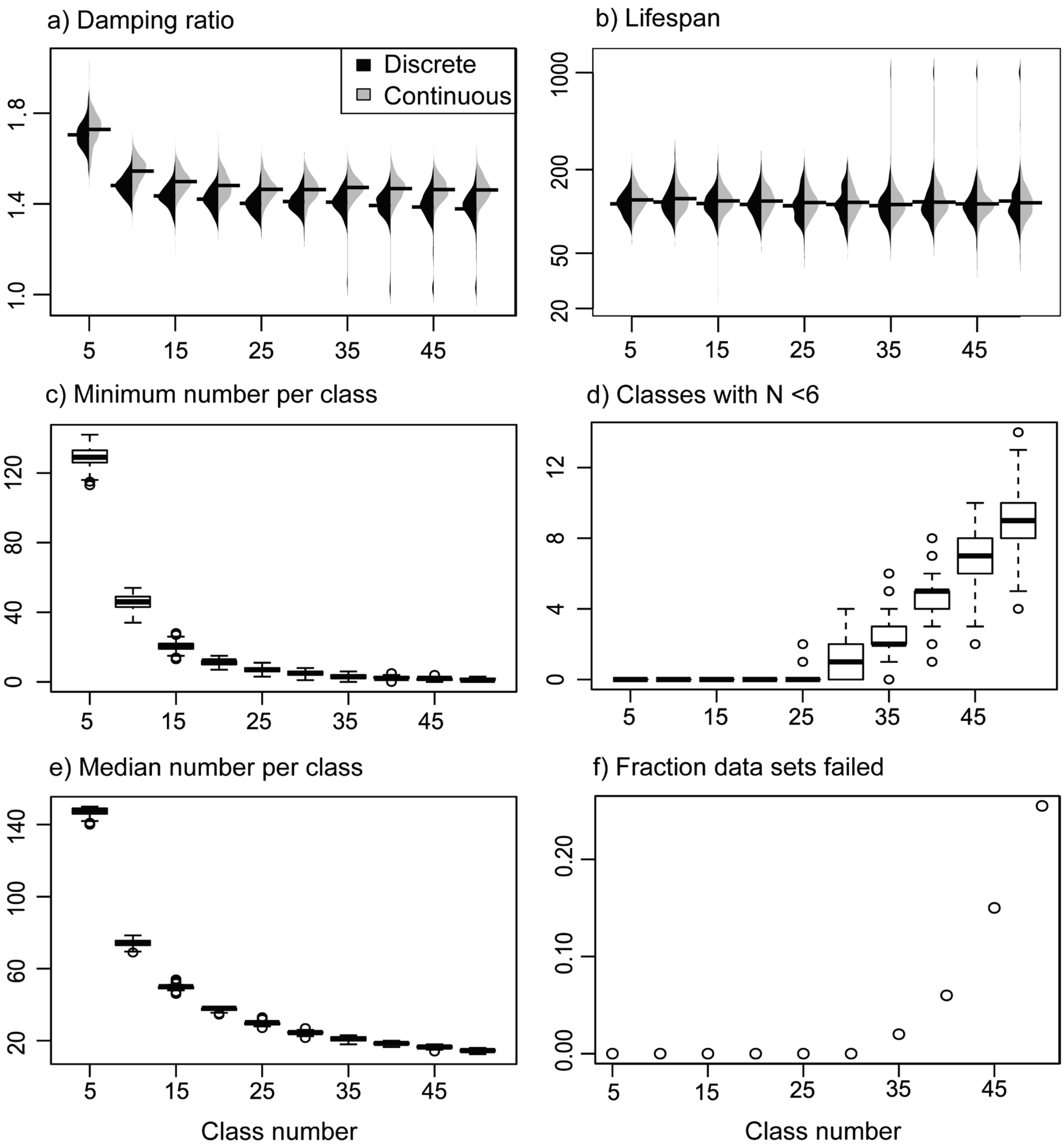

Figure S21. Additional results from rarified bootstraps for bistorts to examine effects of size-class sample sizes (see Figure 15 for lambda results).

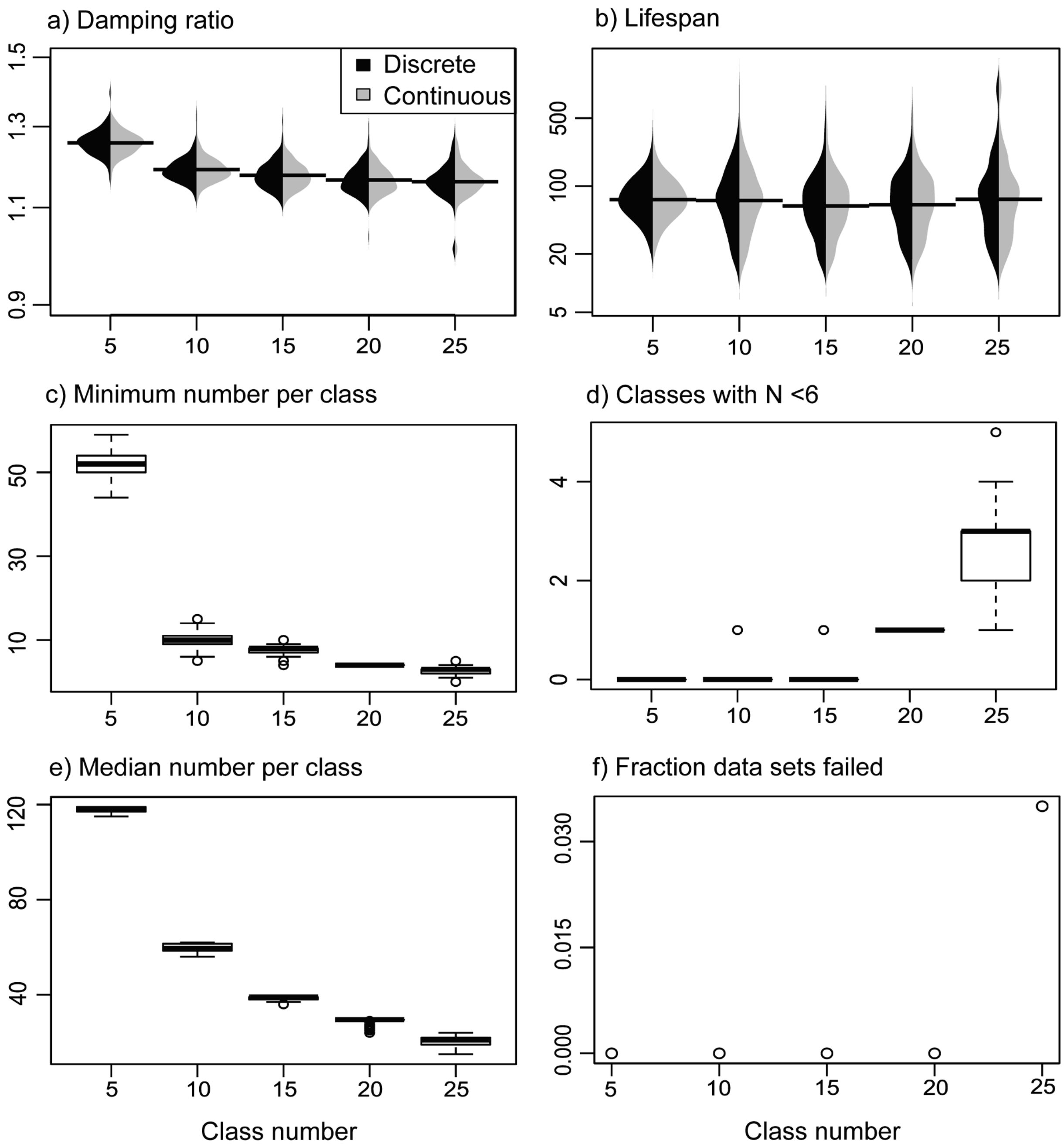

Figure S22. Additional results from rarified bootstraps for *Borderea* to examine issues of size-class sample sizes (see Figure 15 for lambda results).

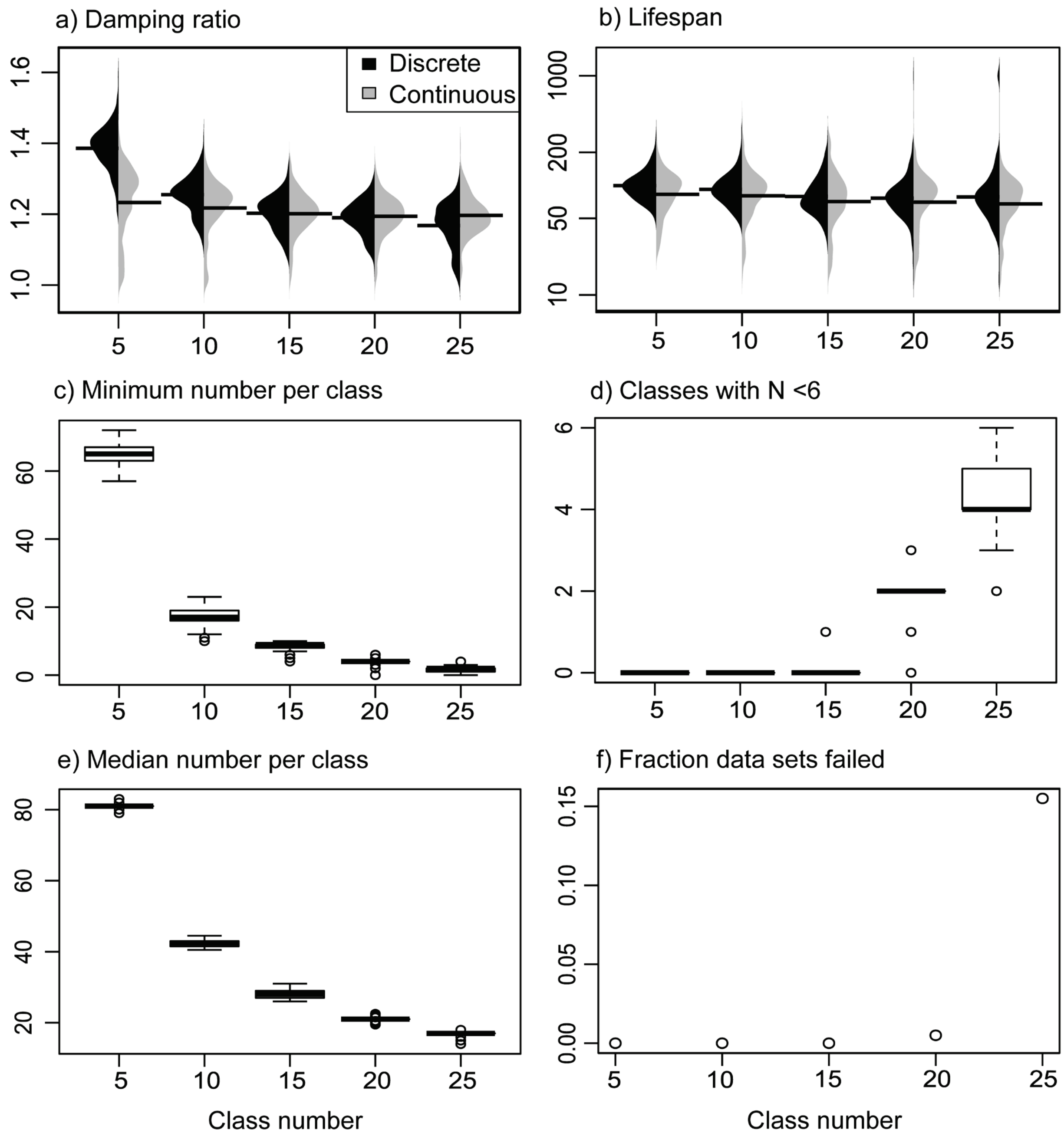

Figure S23. Additional results from rarified bootstraps for *Vulpicida* to examine issues of size-class sample sizes (see Figure 15 for lambda results).

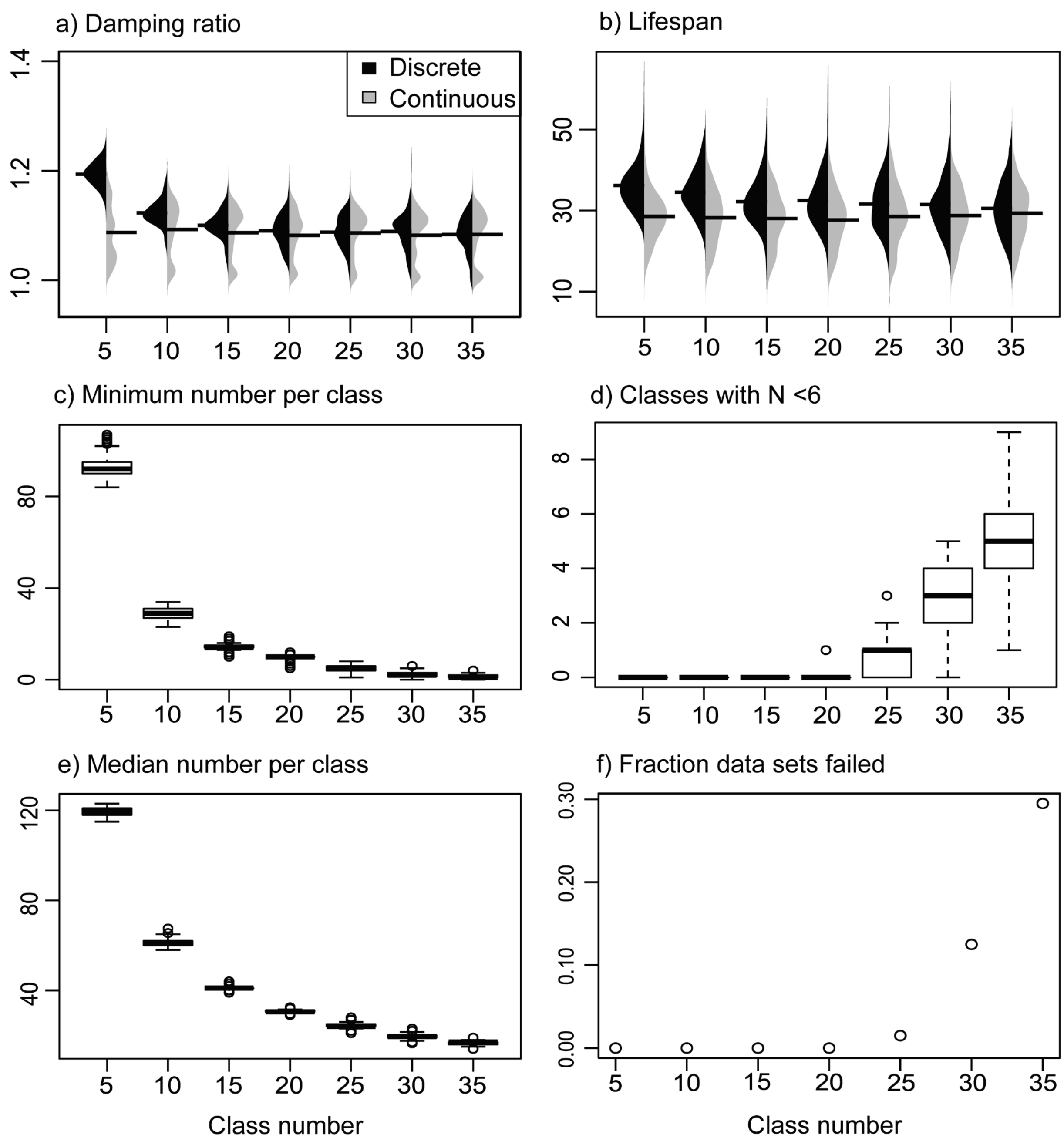

Figure S24. Additional results from rarified bootstraps for gorgonians to examine issues of size-class sample sizes (see Figure 15 for lambda results).

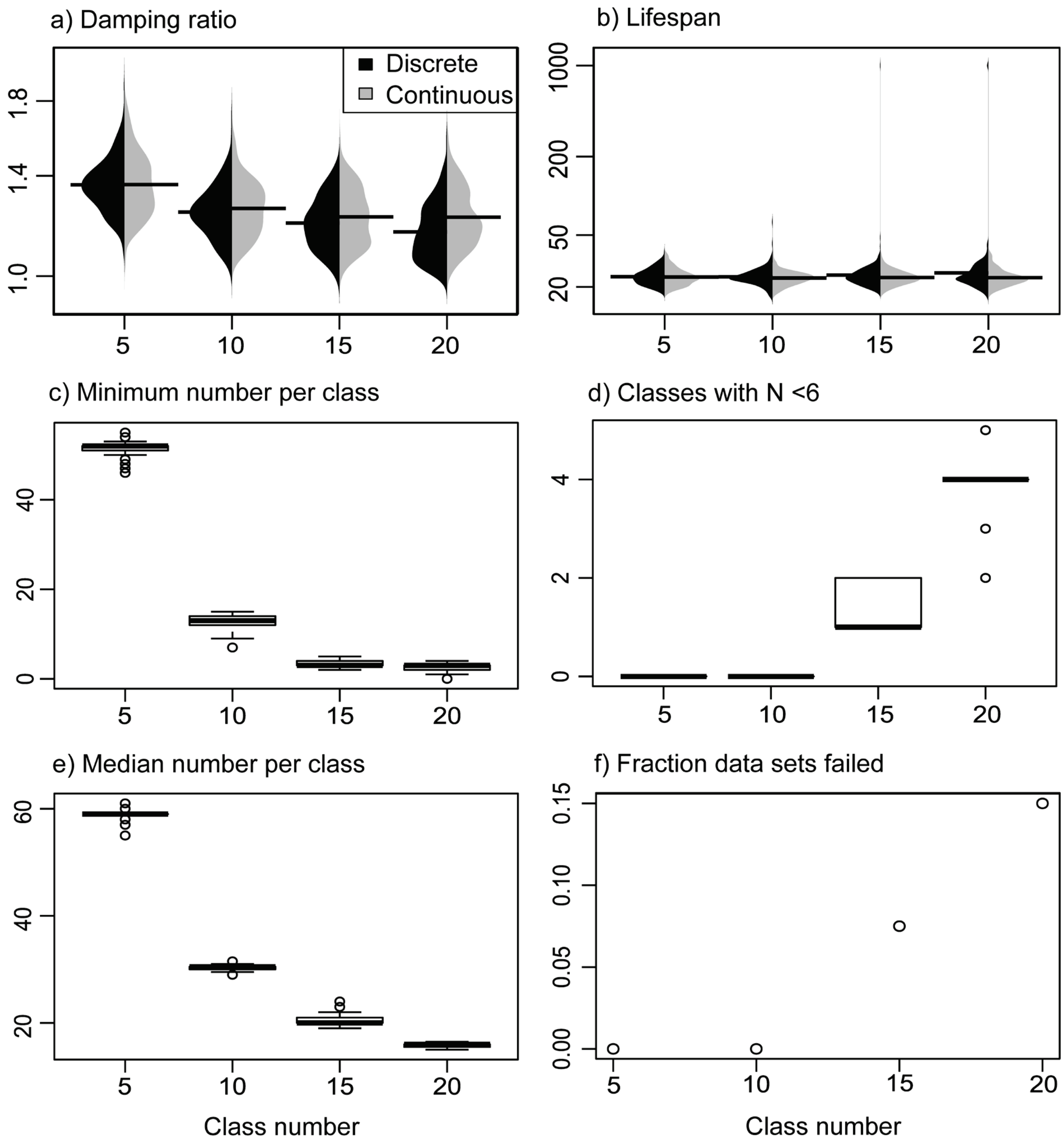

Figure S25. Additional results from rarified bootstraps for guppies to examine issues of size-class sample sizes (see Figure 15 for lambda results).

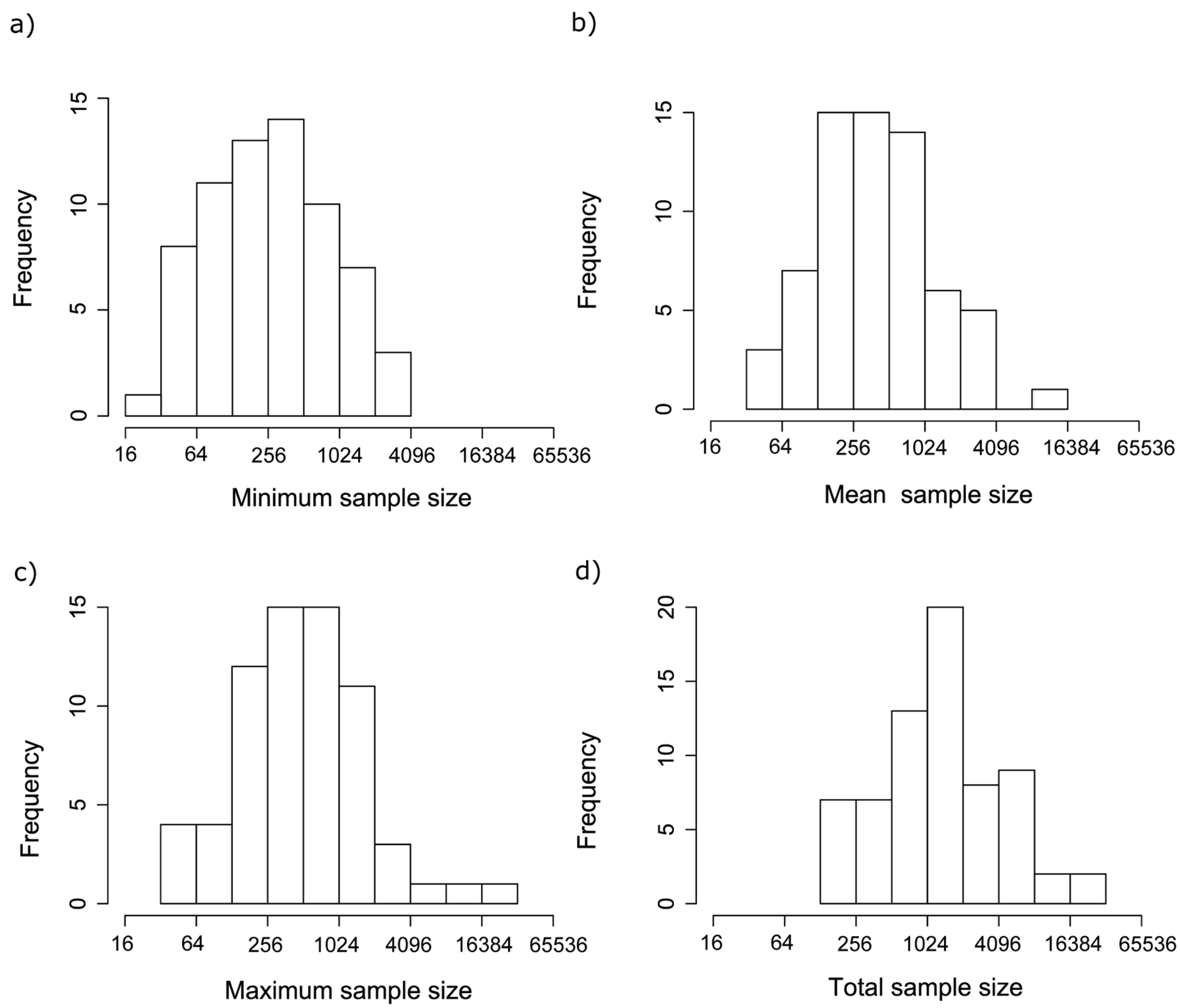

Figure S26. Histograms of sample size statistics for size-based matrix models with discrete vital rate estimation found in literature review. Note the non-linear scaling of sample sizes, used to better visualize lower values. See Fig. S2 legend for details of sample size estimation.